Strojniški vestnik - Journal of Mechanical Engineering 66(2020)5, 289-299,

DOI:10.5545/sv-jme.2019.6523 Original Scientific Paper
Received for review: 2019-12-19
Received revised form: 2020-04-02
Accepted for publication: 2020-04-15

Analysis of the Screening Accuracy of a Linear Vibrating Screen with a Multi-layer Screen Mesh

Hongwei Yan – Yajie Li – Fei Yuan – Fangxian Peng – Xiong Yang – Xiangrong Hou
North University of China, School of Mechanical Engineering, China

This paper investigates the screening characteristics of the multi-layer vibrating screens. A portable linear screen with a three-layer screen mesh and the vibrating screening experimental platform were designed and simulated. Based on the discrete element method (DEM), the influences of the motor excitation frequency, the pulverized coal mass flow rate, and the shape of the particles on the screening accuracy of each layer of the screen and the total energy contained in the particles were analysed. The simulation analysis found that, during the vibration screening process, with the increase of the frequency of motor excitation, the screening accuracy of each screen layers increased first and then decreased. The ratio of the sieving accuracy of the first screen and the third screen is reduced first and then increased. The energy contained in the particles gradually increases. With the increased pulverized coal mass flow rate, the screening accuracy of each layer gradually decreased, while the ratio of the screening accuracy of the first layer to that of the third layer gradually increased. The energy contained in the particles gradually decreases. Similarly, the increased percentage of non-spherical particles generated slightly decreased screening accuracy and an increased ratio of the screening accuracy of the first and third screens. The particles also contain much less energy than spherical particles do. A simulation was carried out on the vibrating screening experimental platform with screening materials such as soybeans and red beans. The experimental results matched the discrete element simulation. The screening accuracy was proved to be higher when the excitation frequency lay in 18 Hz to 20 Hz, and the particles mass flow rate stayed below 0.4 kg/s. This study demonstrated that changing the shape of particles is a practical way of managing real screening work. It also provided a theoretical basis and reference for the design and applications of multi-layer vibrating screens.

Keywords: vibration sieve, discrete element method, screening accuracy, excitation frequency, mass flow rate, particle shape

Highlights

- *According to the design requirements, a three-layer linear vibrating screen is established.*
- *Taking the excitation frequency, the mass flow rate and the shape of particles as variables, the screening accuracy of the vibrating screen is simulated and analysed by using the discrete element method and verified by experiments.*
- *This paper analyses the screening efficiency, the ratio of the first screen to the third screen, and the energy content of particles.*
- *Adjusting the proportion of non-spherical particles can make the simulation results closer to the actual working process.*
- *The results show that the optimum excitation frequency is 18 Hz to 20 Hz, and the maximum mass flow rate is less than 0.4 kg/s.*

0 INTRODUCTION

A linear vibrating screen has many advantages, such as large material handling capacity, long service life, easy maintenance, etc. It has been widely used in coal mining, the chemical industry, the medical industry, etc., [1] and [2]. With the increasing accuracy requirements for screening materials, existing vibrating screens (such as ZKB-type vibrating screens) have been unable to meet current production needs because of its single motion trajectory and low screening accuracy, [3] and [4]. Therefore, it is necessary to explore a new method to simulate and analyse the running state of material particles on the vibrating screen for the problem of the low screening efficiency of current vibrating screens.

The discrete element method (DEM) was first proposed by Cundall [5] and [6], of the Royal Academy of Engineering and American Academy of Engineering, based on the principle of molecular dynamics in 1971. It is an analytical method for discrete granular materials. Its basic idea is to treat the whole medium as composed of a series of discrete and independent particle elements, which have certain geometric, physical, and chemical characteristics; motion is controlled using a conventional motion equation. The deformation and evolution of the whole medium are described by the movement and position of each element. By tracing and calculating the micro-motion of each element, the macro-motion law of the whole research object can be obtained.

At present, the research mainly takes the traditional single-layer screen vibrating screen as the research object and develops the related screening accuracy theory. Zhao et al. [7] and [8] carried out a three-dimensional discrete element simulation on the vibrating screening process to study the influence of the vibration parameters of the vibrating screen on the screening efficiency of the material during the screening process. Li et al. [9] and [10] proposed

*Corr. Author's Address: North University of China, School of Mechanical Engineering, Taiyuan, China, aweigeyan@nuc.edu.cn

that the increase of vibration intensity can improve the screening efficiency of materials to a certain extent but would also increase the loss of materials during the screening process. Elskamp and Harald [11] and [12] conducted vibratory screening research on materials with different particle sizes and shapes. It was found that when the horizontal velocity component of the material is higher than the vertical velocity component, the screening accuracy of the material is higher; otherwise, the screening accuracy is reduced. Dong and Yu [13] studied the influence of the size and shape of the vibrating screen pore on the screening efficiency and analysed the screening of materials under different geometric parameters of the vibrating screen.

Suitable motor excitation frequency and the mass flow rate of the particles can improve the screening accuracy, and it is also an important parameter to measure the screening accuracy of the vibrating screen. Therefore, the linear vibrating screen is taken as the research object, with the shape of material particles, the mass flow rate and the excitation frequency of motor as the control variables. The discrete element method is used to simulate and analyse the influence law of the screening precision of each layer of sieve, which provides a reference for further understanding the screening mechanism of the particle group on the multi-layer sieve vibrating screen.

1 STRUCTURAL DESIGN OF LINEAR VIBRATING SCREEN

Based on the traditional ZKB vibrating screen, an optimization scheme is proposed to design a portable linear vibrating screen containing a multi-layer screen. The structure is mainly composed of a sieve hopper, a screen frame, a column, a screening motor and a screen, and is fixed on the bottom plate. Fig. 1 shows the three-dimensional model of the vibrating screen.

The two screen motors are arranged on both sides of the vibrating screen, and the output end is connected to the eccentric wheel with eccentric block. The eccentric wheel rotation generates a certain intensity of exciting force. The component forces parallel to the direction of the screen offset each other, while the component forces perpendicular to the direction of the screen are superimposed on each other, to increase the throwing index of the vibrating screen and improve the vibration intensity.

Based on the theory of dynamic balance and Lagrange dynamics theory analysis, it is concluded that the spatial motion trajectory of any point on the vibrating screen is like an ellipse, and the relationship between the stiffness of the supporting spring and the relative sensitivity of the screen vibration is analysed, [14] and [15]. The geometric parameters of this vibrating screen member are shown in Table 1.

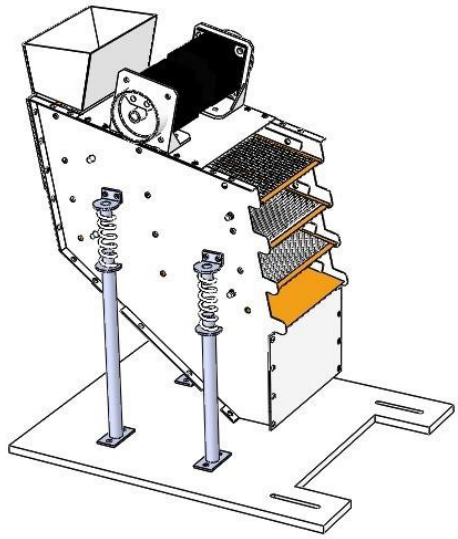

Fig. 1. *Portable linear vibrating screen model*

Table 1. *Shaker design size parameters*

Name	Geometric parameters [mm]
Total length	390
Total width	310
Total height	417
Screen length	300
Screen width	150
Eccentric radius	12
Front pillar height	180
Rear pillar height	224

2 DISCRETE ELEMENT MODEL

In this paper, the discrete element method is used to simulate the motion of particles on a vibrating screen. Its parameter input includes the physical properties of particles and geometry, the contact model, etc. [16] and [17].

First, the geometry model is imported, and the material properties of the pulverized coal particles and the screen are input, as shown in Table 2.

The factors affecting the accuracy of the sieve are mainly the shape, size, concentration ratio, mass flow rate, related geometric parameters, and related geometric parameters, including excitation frequency, vibration direction angle, etc.

According to Zhang [18] and [19], the research on the effect of coal crushing found: the particle size

Table 2. *Material property parameter*

Item	Density [kg/m³]	Elastic recovery coefficient	Static friction factor	Rolling friction factor	Poisson's ratio	Shear modulus [GPa]
Pulverized coal	1300	0.5	0.6	0.05	0.3	1
Screen	7861	0.5	0.4	0.05	0.29	79.9

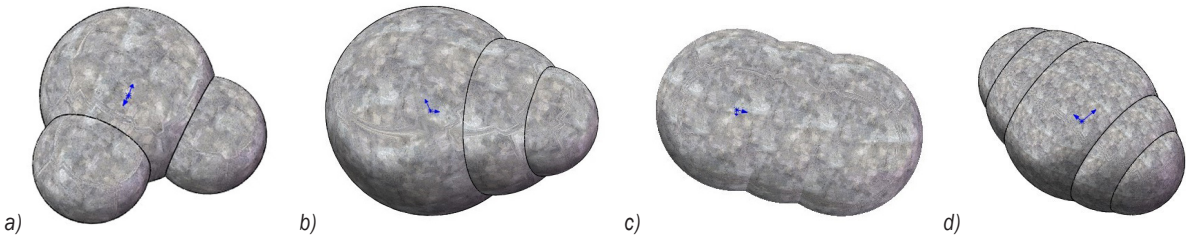

Fig. 2. *Non-spherical particle model; a) 0.7 mm; b) 1.4 mm; c) 2.8 mm; and d) 5 mm*

of coal powder crushing is mostly concentrated in 0.5 mm to 5 mm. Therefore, the screen mesh size is set to 5 mesh, 10 mesh, and 18 mesh in the design process of the vibrating screen, respectively. The relative particle size (the ratio of particle size to mesh size) is 0.7. Therefore, the pulverized coal particles are set to spherical particles of 0.7 mm, 1.4 mm, 2.8 mm, and 5 mm, respectively. The concentration ratio is 1:1:1:1, and the total mass is set to 0.3 kg. The vibration form of the vibrating screen is simplified as follows: the amplitude is 1.5 mm, the swing angle is 0.5°, and the vibration direction angle is 45°.

To simulate the screening situation as well as possible, four kinds of particles were structurally improved, and their corresponding aspheric particle models were designed. The method of equivalent radius is chosen as the method of equivalent volume radius, with which spherical particles and non-spherical particles have the same volume, different shapes, but equal mass **[20]**. Fig. 2 shows four non-spherical particle models.

At present, particle contact models are mainly divided into hard sphere model and soft sphere model. The hard sphere model does not consider the deformation of particles. It is described by the coefficient of recovery and the coefficient of friction. Based on the law of momentum conservation, the integral result of force to time is described as the velocity change before and after particle collision. It is mainly used in the numerical model of fast motion and low concentration particle system.

The model simplifies the contact force between particles by elastic and damping coefficients and calculates the contact force according to its normal overlap and tangential displacement. Thus, the velocity variation of particles can be obtained, which is more suitable for the numerical simulation of engineering problems. The soft sphere model uses the elastic and the damping coefficient to simplify the contact force between the particles. The contact force is calculated according to the normal overlap amount and the tangential displacement, so that the velocity variation of particles can be obtained, which is more suitable for numerical simulation of engineering problems.

Therefore, the soft sphere model is used to simulate the collision behaviour between particles in the screening process, **[21]** and **[22]**. Its mathematical model is shown in Fig. 3.

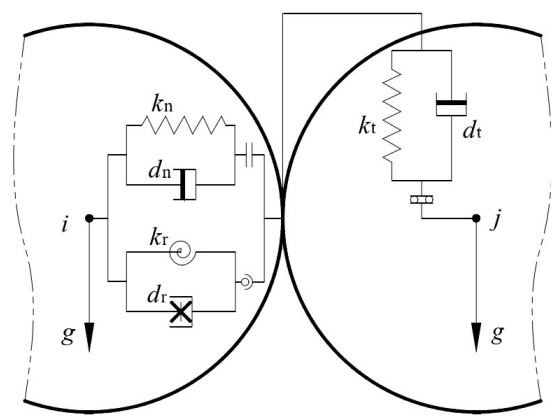

Fig. 3. *Soft particle contact model*

where d_n is normal damping, k_n is normal stiffness, d_t is tangential damping, k_t is tangential stiffness, d_r is rolling damping, and d_k is rolling stiffness.

According to the theory of the mechanics of particulate matter, the motion analysis equation of the i^{th} particulate matter can be expressed as follows:

$$m_i \frac{dv_i}{dt} = m_i g + \sum_{j=1}^{n_i} \left(F_{n,ij} + F_{t,ij} \right),$$

$$I_i \frac{d\omega_i}{dt} = \sum_{j=1}^{n_i} \left(T_{t,ij} + T_{r,ij} \right),$$

where m_i is the mass of inertia of spherical particles, I_i is the and moment of inertia of spherical particles, n_i is the total number of spherical particles, v_i is the movement speed of material particles, and ω_i is the rotational angular velocity of material particles.

Among them, $F_{n,ij}$ (the normal force), $F_{t,ij}$ (the tangential force), $T_{t,ij}$ (the tangential moment), $T_{r,ij}$ (the friction torque) can be obtained according to the theory of mechanical properties of granular materials, **[23]** and **[24]**.

3 SIMULATION ANALYSIS

The movement state of the material particles on the vibrating screen is as follows: when the screening starts, four kinds of material particles are generated in a certain proportion in the granular factory. When the motor rotates at a certain frequency, the vibrating screen also periodically vibrates, the material particles on the net are thrown forward. Under the dual effects of the excitation force and gravity, the particles and the screen frame come into contact and collide to generate energy exchange, which causes the particles to move relative to each other. Particles with a particle size smaller than the mesh size of the screen are screened, while particles having a larger particle size remain on the screen surface until they exit the discharge port. Fig. 4 shows the screening status of the vibrating screen in the simulation.

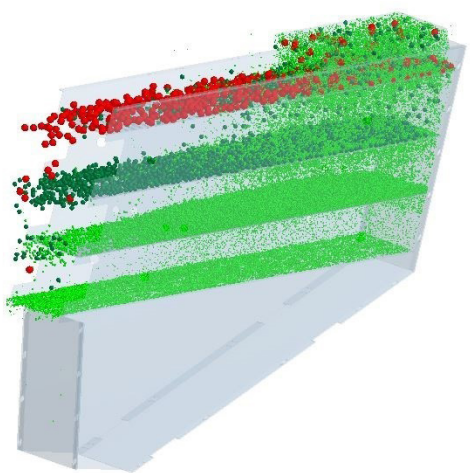

Fig. 4. *Simulating the screening process of vibrating screen*

This paper mainly analyses the running state of material particles on the vibrating screen, taking the motor vibration frequency, particle mass flow rate and its shape and concentration ratio as the control variables, taking the screening accuracy of each screen layer and the ratio of the screening accuracy of the first layer to the third layer as the research variables, and the scheme with the highest screening accuracy under this condition is selected.

3.1 Influence of Vibration Frequency on Screening Accuracy

The vibration frequency of the motor affects the transmission capacity of the vibrating screen and affects the stability of the particle flow screening. According to the discrete element simulation analysis, the screening accuracy of each screen layer is changed, as shown in Fig. 5, under different vibration frequencies.

From Fig. 5, it can be seen that with the increase of motor vibration frequency, the screening accuracy of each screen layer increases first and then decreases. When the vibration frequency is 16 Hz, the screening accuracy of the first layer screen is the highest, reaching 95.6 %; when the vibration frequency is 18 Hz, the screening accuracy of the second layer and the third layer screen is the largest, respectively 94.5 % and 91.2 %. Under the same vibration frequency, the screening accuracy of each screen layer is also different. The screening accuracy of the upper screen is always slightly higher than the screening accuracy of the lower screen. This is because the first screen is screened by four different particle sizes, while the third screen only screens particles with the smallest size, so the first layer screen has higher screening accuracy than other screens. The screening precision ratio of the first layer screen and the third layer screen is as shown in Fig. 6.

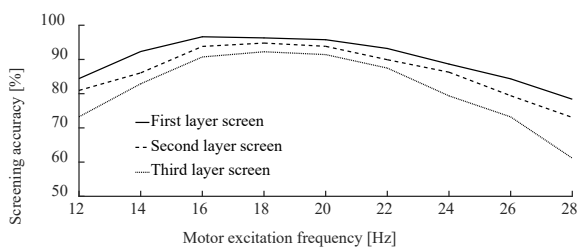

Fig. 5. *Relationship between excitation frequency and screening accuracy*

It can be seen from Fig. 6 that as the vibration frequency of the motor increases, the ratio of the

screening accuracy of the first layer screen and the third layer screen decreases first and then increases. When the vibration frequency is 18 Hz, the ratio of the screening accuracy of the first layer to the third layer is at least 1.04. Currently, the screening accuracy of each layer of the screen is also relatively high. As can be seen from Fig. 6, when the vibration frequency of the motor is too low or too high, the shielding precision of each layer of the screen is relatively low, and the shielding precision ratio of each layer of the screen is also large. The reason for this phenomenon is shown in Fig. 7.

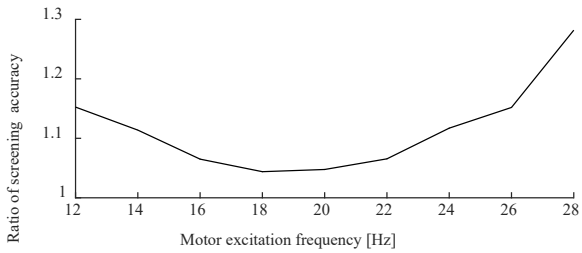

Fig. 6. *Relationship between excitation frequency and screening accuracy ratio*

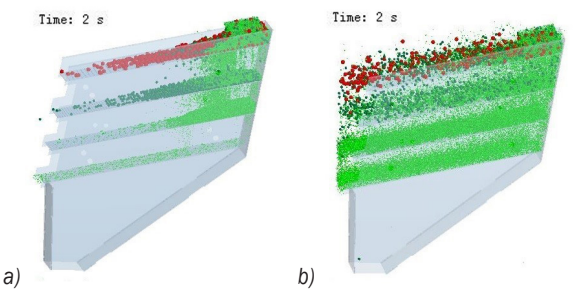

Fig. 7. *Schematic diagram of pulverized coal screening at different frequencies; a) f = 12 Hz; and b) f = 28 Hz*

Fig. 7 shows the vibration screening state of the 2 s time node. It can be seen in Fig. 7 that when the motor vibration frequency is as low as 12 Hz, the material particles cannot obtain energy through contact collision, and it is difficult to be effectively thrown loose. There is a large amount of material at the inlet of each layer of the screen, severely hindering its passage. When the motor vibration frequency is as high as 28 Hz, the particles collide violently, get too much energy, make it fly about in the air, fill the vibrating screen and even fly away from the screening area, greatly reducing screening accuracy.

From an energy point of view, when the excitation frequency is 12 Hz, most 5 mm particles remain on the upper sieve within the specified sieving time. The particles have no or only a small amount of energy and are difficult to move. As the frequency increases, the energy contained in the particles gradually increases, indicating that the collision between particles is intensified, and the screening process can be completed, and the screening time is gradually shortened. When the excitation frequency is increased to 24 Hz, because the excitation frequency is too large, the particles collide violently, the energy obtained is also large, and the screening time is also significantly shortened. However, a large number of small particles come out of the screen in advance with the large particles, and the screening efficiency is greatly reduced.

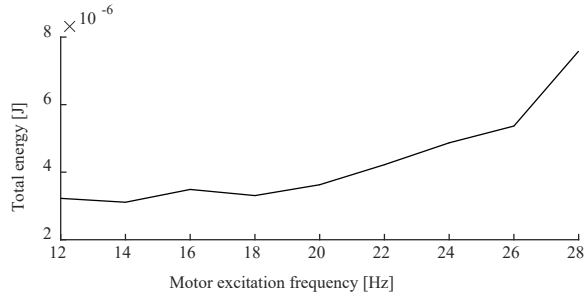

Fig. 8. *Energy relationship of particles at different excitation frequencies*

Therefore, the optimal excitation frequency is about 16 Hz to 20 Hz.

3.2 Influence of Mass Flow Rate on Screening Accuracy

During the screening process, different mass flow rates are bound to have an impact on the screening accuracy of the pulverized coal on each layer of the screen. According to the discrete element simulation analysis, the relationship between different mass flow rates and the screening accuracy of each layer of mesh is shown in Fig. 9.

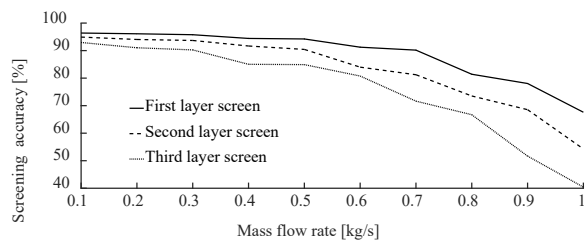

Fig. 9. *Relationship between mass flow rate of pulverized coal and screening accuracy*

It can be seen from Fig. 9 that as the mass flow rate of the pulverized coal increases, the screening accuracy of each layer of the screen is accelerated to decrease. When the mass flow rate of pulverized coal

is 0.1 kg/s, the screening accuracy of the first layer screen is the highest, at about 96.38 %. When the mass flow rate is 1 kg/s, the screening accuracy of the third layer screen is the lowest, about 42.41 %. This is because when the mass flow rate of the pulverized coal is small, the amount of pulverized coal flowing into the screen at the same time is small, and the pulverized coal can be sufficiently thrown under the action of the exciting force, thereby facilitating the sieving of the pulverized coal. When the mass flow of pulverized coal is large, more pulverized coal flows into the screen at the same time, which is not conducive to the loosening of the pulverized coal by contact collision, which, in turn, is not conducive to the sieving of coal powder. When the mass flow rate of pulverized coal is constant, the screening accuracy of each screen layer is also that the screening accuracy of the upper screen is slightly higher than that of the lower screen. The screening accuracy ratio of the first layer screen and the third layer screen is as shown in Fig. 10.

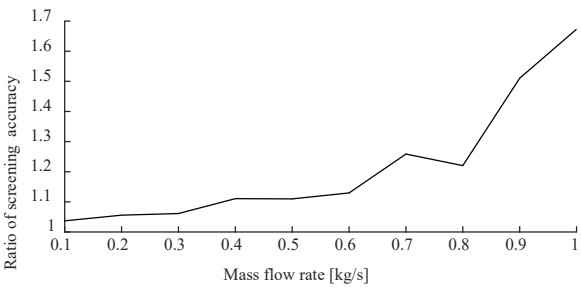

Fig. 10. *Relationship between mass flow rate and screening accuracy ratio*

It can be found from Fig. 10 that as the mass flow rate of pulverized coal increases, the ratio of the screening precision of the first layer of the screen to the third screen layer increases gradually, from about 1.037 to about 1.657. When the mass flow rate reaches about 0.6 kg/s, the total amount of coal powder on the screen exceeds the maximum processing capacity of the screen, and the first screen layer has obvious clogging phenomenon, as shown in Fig. 11.

When the mass flow rate of pulverized coal is large, there is more coal powder flowing into the screen at the same time. While the pulverized coal is thrown up, a large amount of pulverized coal still flows into the inlet of the vibrating screen.

Due to the limited screening space, the pulverized coal originally thrown up is pressed downward, and the mass flow rate is large, the processing capacity of the screen is limited, and the material accumulation and overflow are easily caused, so that the smaller pulverized coal particles do not have enough space to move towards the outlet of the screen mesh, which is not conducive to the screening of materials.

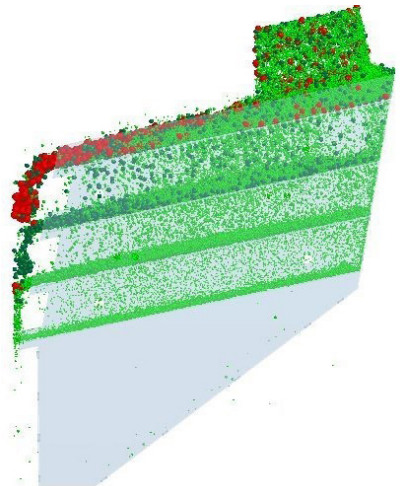

Fig. 11. *Screen mesh blocking diagram*

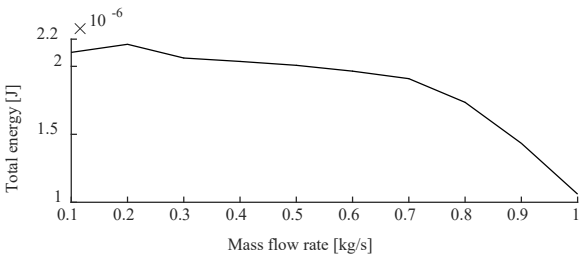

Fig. 12. *Energy relationship of particles at different mass flow rates*

From the energy point of view, when the mass flow rate is small, the particle energy is large, and the change is relatively gentle. As the particle mass flow rate increases, the energy contained in the particles gradually decreases, and the rate of decrease increases. This also shows that when the mass flow rate is small, the particles can be fully sieved, the collision between the particles is more violent, the energy contained is larger, and the time used for sieving is also relatively short. As the mass flow rate increases, more pulverized coal particles flow at the same time. Due to the limited sieving space, the pulverized coal that was originally thrown upward was pressed down, which greatly reduced the contact and collision between particles. As a result, the sieving time is prolonged, and the reason for the accelerated reduction of the energy contained in the particles is explained.

Therefore, without affecting the normal use of the vibrating screen, the mass flow rate of the particles should not exceed 0.4 kg/s.

3.3 Effect of Particle Shape and Concentration Ratio on Screening Accuracy

The simulation settings are as follows: 25 % of 0.7 mm particles, 25 % of 1.4 mm particles, 25 % of 2.8 mm particles, 25 % of 3.5 mm particles. A total of three simulations were performed: 100 % spherical particles, 50 % spherical particles and 50 % non-spherical particles, and 100 % non-spherical particles. Fig. 13 shows the variation of the screening accuracy of each screen layer under three working conditions.

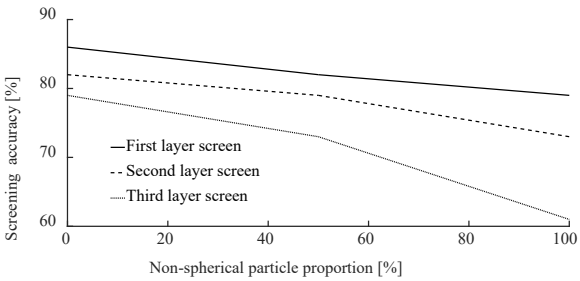

Fig. 13. *Effect of particle shape on screening accuracy*

It can be seen from Fig. 13 that with the increase of the proportion of non-spherical particles, the overall screening accuracy of each screen layer shows a downward trend. When the proportion of non-spherical particles is 0, the screening accuracy of each layer is the highest, which is 95.6 %, 94.5 % and 91.2 % respectively. When the proportion of the non-spherical particles is 100 %, the screening accuracy of the first layer of the screen does not have much influence, and the screening accuracy of the second and third layers of the screen is reduced more. This is because the shape of the non-spherical particles is irregular, and it is easier to block them at the mesh of the screen, and the collision between the particles is intensified, so that the small particles are screened in advance, which greatly reduces the screening accuracy. The screening accuracy ratio of the first layer screen and the third layer screen is as shown in Fig. 14.

It can be seen from Fig. 14 that as the proportion of non-spherical particles increases, the ratio of the screening precision of the first layer screen to the third layer screen gradually increases. When the sieved particles are all non-spherical particles, the ratio of the first layer screen to the third layer screen is the largest, and the ratio is 1.281. At this time, small particles are screened in advance with large particles in the upper screen, resulting in a slight reduction in the screening accuracy of the upper screen, and a significant reduction in the screening accuracy of the lower screen.

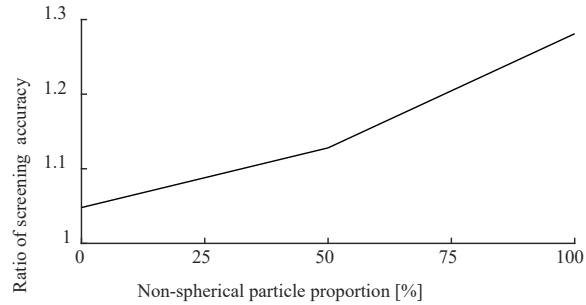

Fig. 14. *Relation between particle shape and screening accuracy ratio*

Table 3. *Influence of particle shape and energy content*

Proportion of non-spherical particles [%]	0	50	100
Total energy $\times 10^{-6}$ [J]	3.43	2.16	1.05

From an energy point of view, during the sieving process, the energy obtained by spherical particles is greater than that obtained by non-spherical particles. This is because spherical particles are more uniform, energy exchange is more likely to occur during collision, and it is easier to pass through the screen. The shape of non-spherical particles is more complicated, and they are easily affected by the current attitude during the collision process, and their edges and corners often prevent them from passing through the screen, causing most of the energy obtained to be dissipated.

In summary, the shape of the material particles has a certain influence on the simulation results when using the discrete element method for simulation analysis.

4 ANALYSIS OF VIBRATION SCREENING EXPERIMENT

An experimental platform for vibration screening was built. The screening accuracy of each screen layer was analysed experimentally with the excitation frequency of the motor and the mass flow rate of the particles. The results of the simulation and experiment verify each other, which can provide a basis for the structural optimization design of linear vibration screen and the application and development of the discrete element method.

4.1 Preparation in Advance

Firstly, an experimental platform is built to prepare the raw materials for the experiment, to simulate the

screening process. Millet, red bean, rice and soybean were selected as screening materials to simulate different shapes of material particles. Different raw materials were mixed evenly at the ratio of 1:1:1:1 using an electronic scale, and each material used for screening was 0.3 kg. To reduce the impact of contingency factors on the experimental results, 30 samples of the above 0.3 kg particles were prepared, and repeated experiments were carried out. Fig. 15 shows all the experimental conditions prepared.

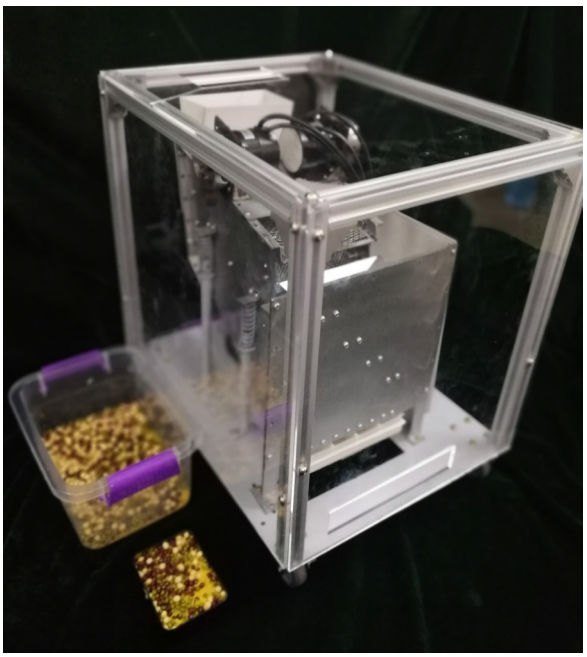

Fig. 15. *Linear vibrating screen test platform*

4.2 Experimental Process

In this experiment, the excitation frequency of the motor and the mass flow rate of the particles are taken as the research objects. When setting the parameters of excitation frequency, the minimum excitation frequency is 12 Hz, i.e., the motor speed is 720 r/min, and the increase of 2 Hz, i.e. 120 r/min, is selected to control the variable experimental analysis. When setting mass flow rate parameters, a certain amount of material is prepared in advance and placed in the bin. All materials in the cartridge are poured into the hopper of sieve feeder within 1 to 3 seconds to simulate different mass flow rates.

In the course of the experiment, a certain number of particles is used as a test quantity, and about 10 repeated experiments are carried out. The maximum and minimum values of the experimental results are removed, and the remaining results are averaged as the results, and then the data are analysed.

4.2.1 Experimental Study on the Effect of Exciting Frequency on Screening Accuracy

The influence of the excitation frequency of the motor on the screening accuracy of the vibration screen is analysed by using the control variable method. The experimental results are shown in Fig. 16.

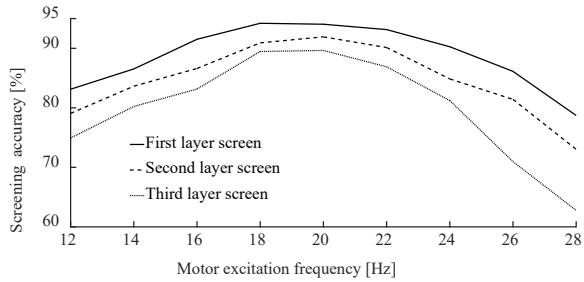

Fig. 16. *Experimental relationship between frequency and screening accuracy*

It can be found from Fig. 16 that as the excitation frequency increases, the sieving accuracy of each layer of sieve screens first increases and then decreases. The screening accuracy of the upper screen is always greater than the screening accuracy of the lower screen. When the excitation frequency is 18 Hz to 20 Hz, the screening accuracy of each layer of sieve reaches the highest. When the excitation frequency is greater than 24 Hz, due to the violent contact and collision between particles, some particles fly away from the screen, and the screening accuracy of each layer of the screen is rapidly reduced. The particle size of the third layer of the screen is the smallest, and the screening accuracy is also the fastest. The relationship between the excitation frequency and the screening accuracy is shown in Fig. 17.

From Fig. 17, it can be found that with the increase of excitation frequency, the ratio of screening accuracy of the first layer screen to that of the third layer screen decreases first and then increases. When the excitation frequency is 20 Hz, the ratio is about 1.06. When the excitation frequency is less than 24 Hz, the ratio of screening accuracy changes more gently. When the excitation frequency exceeds 24 Hz, the screening accuracy of the screen changes dramatically. This is due to the high frequency of excitation and the small size of pulverized coal particles, because of their small mass and inertia, are more vulnerable to impact and fly out of the screen area in the severe contact impact environment. Currently, the screening

accuracy of the first layer sieve decreases slowly while that of the third layer sieve decreases greatly, which makes the ratio of the first layer sieve to the third layer sieve increase rapidly.

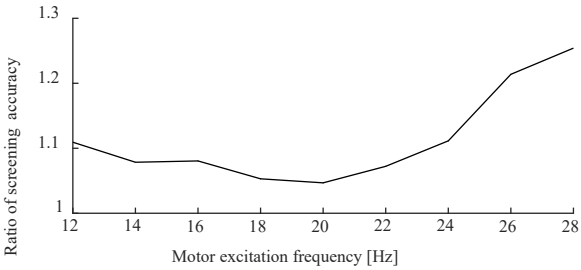

Fig. 17. *Experimental diagram of the ratio of frequency to screening accuracy*

4.2.2 Experimental Study on the Effect of Mass Flow Rate on Screening Accuracy

Studying the influence of pulverized coal mass flow rate on the screening accuracy of vibrating screen can in further understanding the screening capacity of this vibrating screen, and provide a basis for more effective and rational use of vibrating screen. The experimental results are shown in Fig. 18.

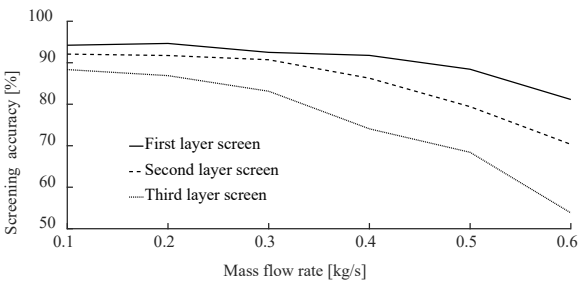

Fig. 18. *Experimental diagram of the relationship between mass flow rate and screening accuracy*

It can be found from Fig. 18 that with the increase of the pulverized coal mass flow rate, the sieving accuracy of the sieves of each layer is continuously decreasing. The screening accuracy of the upper screen is always greater than the screening accuracy of the lower screen. When the mass flow rate is less than 0.4 kg/s, the working state of the vibrating screen is relatively stable, and the screening accuracy is good. When the mass flow rate is 0.4 kg/s to 0.6 kg/s, the sieving accuracy of each layer of sieve begins to decrease significantly. When the mass flow rate is greater than 0.6 kg/s, the screening accuracy of the third screen layer is low, and a large amount of accumulation occurs at the feed end, so the analysis of the larger mass flow rate is no longer performed. The ratio of mass flow rate to sieving accuracy is shown in Fig. 19.

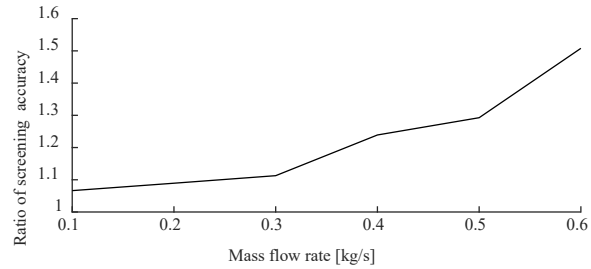

Fig. 19. *Experimental diagram of the ratio between mass flow rate and screening accuracy*

It can be found from Fig. 19 that, with the increase of the mass flow rate of pulverized coal, the ratio of the screening accuracy of the first screen to that of the third screen increases. When the mass flow rate is 0.1 kg/s, the ratio of accuracy is about 1.07, and when the mass flow rate increases to 0.6 kg/s, the ratio reaches 1.51. When the mass flow rate is less than 0.3 kg/s, the ratio of screening accuracy changes more gently, and when the mass flow rate is 0.4 kg/s, the screening accuracy of the screen will change dramatically. In conclusion, within the range of pulverized coal mass flow rate, the screening accuracy of the first and the second screens changes smoothly, while that of the third screens decreases dramatically, resulting in a sharp increase in the ratio of screening accuracy.

5 COMPARATIVE ANALYSIS OF EXPERIMENTAL AND SIMULATION RESULTS

5.1 Simulation and Experimental Analysis of Excitation Frequency

Comparative experiments and simulation results show that when the excitation frequency is 18 Hz to 20 Hz, the screening accuracy of each screen layer is the highest, which is slightly higher than the optimal frequency of 16 Hz to 18 Hz in the simulation. The highest screening accuracy is about 2 % to 4 % lower than the simulation result. The reason for this decrease in accuracy is mainly the difference in the adsorption of fine pulverized coal particles and the different shapes of the particles during the screening process. When the frequency is 18 Hz to 20 Hz, the ratio of sieving accuracy appears the lowest value, and the working condition at this time is the best.

In summary, when the excitation frequency is 18 Hz to 20 Hz, the screening accuracy of each layer of sieve reaches the highest.

5.2 Simulation and Experimental Analysis of Mass Flow Rate

Comparing the experimental and simulation results, it is found that the sieving accuracy of the screens of each layer is lower than the simulation results. Among them, the sieving accuracy of the first layer of sieve has the smallest decrease, about 7 %, and the sieving accuracy of the third layer of sieve has the largest decrease, about 31 %, which also explains why the ratio of sieving accuracy suddenly increases. In addition, the experimental results have a larger decline than the simulation results, which also shows that the actual screening process is more complicated than the simulation results. When the mass flow rate is 0.4 kg/s, the sieving accuracy decreases, but it can still maintain a high state.

In summary, the best mass flow rate to ensure that the vibrating screen can work normally and have high screening accuracy is not more than 0.4 kg/s.

6 CONCLUSIONS

In this study, a portable linear vibrating screen with three layers of screen mesh was designed. DEM was used to analyse the moving characteristics of material particles on the vibrating screen. Then a vibration screening experimental platform was built to run the cross-check of the results. It was shown that:

(1) With increased pulverized coal mass flow rate, the screening accuracy of each screen layer gradually decreased, and the ratio of the screening accuracy of the first screen layer to that of the third screen layer gradually increased. The energy contained in the particles gradually increases.

(2) With increased excitation frequency, the screening accuracy of each screen layer first increased and then decreased, and the ratio of screening accuracy of the first screen layer to that of the third screen layer first decreased and then increased. The energy contained in the particles gradually decreases.

(3) In the simulation process, properly adjusting the proportion of spherical and non-spherical particles can make the simulation results closer to the actual working process, and the conclusions obtained are closer to the actual results.

(4) To achieve the best screening accuracy, the portable linear vibrating screen should be working with the optimum excitation frequency of 18 Hz to 20 Hz, and its maximum mass flow rate should be less than 0.4 kg/s.

7 ACKNOWLEDGEMENTS

The work described in this paper has been supported by the Shanxi Province Natural Science Foundation, China (2013011026-2), it is mainly reflected in the energy-saving and environmental protection aspects of pulverized coal screening; it is a key technology for intelligent production. The research work also received a grant from the Shanxi Province Key Technologies R&D Programme of China (201603D321117). The authors would like to express their gratitude for the support of this study.

8 REFERENCES

[1] Peng, L., Wang, Z., Ma, W., Chen, X., Zhao, Y., Liu, C. (2018). Dynamic influence of screening coals on a vibrating screen. *Fuel*, vol. 216, p. 484-493, **DOI:10.1016/j.fuel.2017.12.04**.

[2] Song, J., Liu, L., Wang, M., Zhang, J. (2017). Improved design and test of 4B-1200 type Bulbus Fritillariae Ussuriensis medicinal materials harvester. *Nongye Gongcheng Xuebao/ Transactions of the Chinese Society of Agricultural Engineering*, vol. 33, no. 01, p. 45-51, **DOI:10.11975/j.issn.1002-6819.2017.01.006**.

[3] Shen, H., Zhu, X., Dai, L., Deng, J. (2014). Design of less-input more-output parallel mechanisms. *Lecture Notes in Computer Science*, vol. 8918, p. 81-88, **DOI:10.1007/978-3-319-13963-0_8**.

[4] Chernova, E.V., Chernov, D.V. (2017). Current status and application of fine screening technology in China. *IOP Conference Series: Earth and Environmental Science*, vol. 87, no. 2, **DOI:10.1088/1755-1315/87/2/022005**.

[5] Cundall, P.A., Strack, D.L. (1979). A discrete numerical model for granular assemblies. *Géotechnique*, vol. 29, no. 1, p. 47-65, **DOI:10.1680/geot.1979.29.1.47**.

[6] Cundall, P.A., Strack, D.L. (1983). Modeling of microscopic mechanisms in granular material. *Studies in Applied Mechanics*, vol. 7, p. 137-149, **DOI:10.1016/B978-0-444-42192-0.50018-9**.

[7] Zhao, L., Zhao, Y., Bao C., Hou, Q, Yu, A. (2016). Laboratory-scale validation of a DEM model of screening processes with circular vibration. *Powder Technology*, vol. 303, p. 269-277, **DOI:10.1016/j.powtec.2016.09.034**.

[8] Zhao, L., Zhao, Y., Liu, C., Li, J., Dong, H. (2011). Simulation of the screening process on a circularly vibrating screen using 3D-DEM. *Mining Science and Technology*, vol. 21, no. 5, p. 677-680, **DOI:10.1016/j.mstc.2011.03.010**.

[9] Li, H., Li, Y., Guo, F., Zhao, Z., Xu, L. (2012). CFD–DEM simulation of material motion in air-and-screen cleaning device. *Computers and Electronics in Agriculture*, vol. 88, p. 111-119, **DOI:10.1016/j.compag.2012.07.006**.

[10] Li, H., Li, Y., Tang, Z., Xu, L., Zhao, Z. (2011). Numerical simulation and analysis of vibration screening based on EDEM. *Transactions of the CSAE*, vol. 27, no. 5, p. 117-121, **DOI:10.3969/j.issn.1002-6819.2011.05.019**.

[11] Elskamp, F., Kruggel-Emden, H. (2018). DEM simulations of screening processes under the influence of moisture. *Chemical Engineering Research and Design*, vol. 136, p. 593-609, **DOI:10.1016/j.cherd.2018.06.022**.

[12] Elskamp, F., Kruggel-Emden, H. (2019). Extension of process models to predict batch screening results under the influence of moisture based on DEM simulations. *Powder Technology*, vol. 342, p. 698-713, **DOI:10.1016/j.powtec.2018.10.039**.

[13] Dong, K.J., Yu, A.B. (2012). Numerical simulation of the particle flow and sieving behavior on sieve bend/low head screen combination. *Minerals Engineering*, vol. 31, p. 2-9, **DOI:10.1016/j.mineng.2011.10.020**.

[14] otich, N., Tuunila, R., Elkamel, A., Louhi-Kultanen, M. (2017). Dynamic and perturbative system analysis of granular material in a vibrating screen. *Advance Powder Technology,* vol. 28, no. 12, p. 3257-3264, **DOI:10.1016/j.apt.2017.09.031**.

[15] Zhao, Y.M., Liu, C.S., He, X.M., Zhang, C.Y., Wang, Y.B., Ren, Z.T. (2009). Dynamic design theory and application of large vibrating screen. *Procedia Earth and Planetary Science*, vol. 1, no. 1, p. 776-784, **DOI:10.1016/j.proeps.2009.09.123**.

[16] Zhai, Y., Xiong, X., Tang, J. (2019). Impact disaggregation simulation of wet coal agglomerate using Discrete Element Method. *Coal Engineering*, vol. 51, no. 12, p. 167-171, **DOI:10.11799 /ce201912034**.

[17] Dehestani, M., Asadi, A. Mousavi, S.S. (2017). On discrete element method for rebar-concrete interaction. *Construction and Building Materials*, vol. 151, p. 220-227, **DOI:10.1016/j.conbuildmat.2017.06.086**.

[18] Yang, J.,Zhen, K., Ru, Y., Zhang, H. (2018). Study on crushing effect of irregular middlings with different crushing methods. Coal Technology, vol. 37, no. 01, p. 33-35, **DOI:10.13301/j.cnki.ct.2018.01.111**. (in Chinese)

[19] Zhang, F.W., Ru, Y., Zhang, H.J. (2017). Study of crushing effect of coal middlings from vense medium separation based on different crushing modes. *Coal Technology*, vol. 36, no. 02, p. 303-306, **DOI:10.13301/j.cnki.ct.2017.02.119**. (in Chinese)

[20] Sugaya, S., Yamada, M., Seki, M. (2011). Observation of nonspherical particle behaviors for continuous shape-based separation using hydrodynamic filtration. *Biomicrofluidic*s, vol. 5, no. 2, **DOI:10.1063/1.3580757**.

[21] Elghannay, H., Tafti, D., Yu, K. (2019). Evaluation of physics based hard-sphere model with the soft sphere model for dense fluid-particle flow systems. *International Journal of Multiphase Flow*, vol. 112, p. 100-115, **DOI:10.1016/j.ijmultiphaseflow.2018.12.004**.

[22] Sandlin, M., Abdel-Khalik, S.I. (2018). A study of granular flow through horizontal wire mesh screens for concentrated solar power particle heating receiver applications – Part I: Experimental studies and numerical model development. *Solar Energy*, vol. 169, no. 15, p. 1-10, **DOI:10.1016/j.solener.2018.03.036**.

[23] Zhang, W., Zhou, J., Yu, S.W., Zhang, X.J., Liu, K. (2018). Quantitative investigation on force chains of metal powder in high velocity compaction by using discrete element method. *Journal of Mechanical Engineering*, vol. 54, no. 10, p. 85-92, **DOI:10.3901/JME.2018.10.085**. (in Chinese)

[24] Dai, Y., Pang, L.P., Chen, L.S., Zhu, X., Zhang, T. (2016). A new multi-body dynamic model of a deep ocean mining vehicle-pipeline-ship system and simulation of its integrated motion. *Strojniški vestnik - Journal of Mechanical Engineering*, vol. 62, no. 12, p. 757-763, **DOI:10.5545/sv-jme.2015.3211**.